Mathematical Methods in the Applied Sciences

WILEY

RESEARCH ARTICLE

Development of Chelyshkov Wavelets Neural Network Method for Solving Nonlinear Fractal–Fractional Optimal Control Problems

Parisa Rahimkhani[1] | Seydi Battal Gazi Karakoc[2] | Thabet Abdeljawad[3,4,5]

[1]Faculty of Science, Mahallat Institute of Higher Education, Mahallat, Iran | [2]Department of Mathematics, Faculty of Science and Art, Nevsehir Hacı Bektas Veli University, Nevsehir, Türkiye | [3]Department of Fundamental Sciences, Faculty of Engineering and Architecture, Istanbul Gelisim University, Istanbul, Türkiye | [4]Department of Mathematics and Sciences, Prince Sultan University, Riyadh, Saudi Arabia | [5]Department of Medical Research, China Medical University, Taichung, Taiwan

Correspondence: Parisa Rahimkhani (rahimkhani.parisa@gmail.com) | Thabet Abdeljawad (tabdeljawad@psu.edu.sa)

Received: 4 June 2025 | **Revised:** 13 February 2026 | **Accepted:** 1 June 2026

Keywords: Chelyshkov wavelets | convergence analysis | fractal–fractional optimal control problem | neural network method | numerical method

ABSTRACT

This paper employs Chelyshkov wavelets neural network method for solving nonlinear fractal–fractional optimal control problems (FFOCPs) in the Atangana–Riemann–Liouville sense. The described neural network is comprised of three layers: the input layer, the hidden layer, and the output layer. This three-layer structure allows the neural network to learn complex relationships between input and output by applying Chelyshkov wavelets in the hidden layer and nonlinear scaling in the output layer. Initially, the problem under investigation is transformed into an equivalent variational problem by applying the definition of the fractal–fractional integral. Subsequently, by utilizing the Chelyshkov wavelets, the neural network method, and the Gauss–Legendre integration, the problem is reformulated as a system of algebraic equations. Finally, this system is solved using Newton's iterative method. Additionally, we show the convergence of the proposed approach within the Hilbert space framework. To assess the applicability and efficacy of the proposed scheme, four examples are given.

MSC2020 Classification: 26A33, 33F05, 92B20

1 | Introduction

Recently, fractional differential equations (FDEs) and fractional calculus (FC) have attracted considerable attention in science and engineering. The development of FC and FDEs has a long history, dating back to the seminal works of G.W. Leibniz (1695) and L. Euler (1730) in the seventeenth century. FC and FDEs have been used to study a wide range of applied sciences, industrial, and engineering problems in recent decades. For example, viscoelasticity [1], bioengineering [2], econometrics [3], statistical mechanics [4], and solid mechanics [5].

Several definitions of the fractional derivative have been introduced, such as, Caputo fractional derivative, Riemann–Liouville fractional derivative, and Hadamard fractional derivative [6, 7]. Meanwhile, a new derivative operator known as the fractal–fractional (FF) derivative was developed by combining the ideas of the fractal derivative and fractional derivative [8]. The formulation of FF ordering problems can be found in [9, 10]. These sources show that the FF operator order models perform better than the integer order, and [9] shows that these operators are very suitable for solving problems in the actual world. Numerous scientific fields, including banking and finance [11], chaotic diverse problems [12] and Ebola virus simulation [13], have examined FF operators. It is noteworthy that, thus far, a variety of numerical methods have been developed and applied to solve diverse classes of FF differential equations. For instance, Hosseininia et al. [14] solved the FF two-dimensional Emden–Fowler equation via the 2D Chelyshkov polynomials method. Araz [15] proposed a numerical method for FF Volterra integro-differential equation. Rahimkhani et al. [16] applied the Chelyshkov polynomials and the Legendre–Gauss quadrature rule for FF 2D integro-differential equations. Rayal and Verma [17] solved pantograph differential equation of the stretched type associated with FF derivatives via the fractional order Legendre wavelets. Rahimkhani et al. [18] introduced a method based on the Vieta-Fibonacci polynomials FF integral operators for solving FF differential equations system.

A field of mathematics known as "optimal control theory" is concerned with maximizing or minimizing a specified cost function in particular dynamical systems. The fractional optimal control problem (FOCP) is an optimal control problem in which the criterion function or the differential equations governing the dynamics of the system or both contains at least one fractional order derivative term. At present, FOCPs have gained importance due to their many applications in engineering, science, economics, geometry, and many other fields. To mention a few, FOCPs have been used in the materials with memory and hereditary effects, dynamical processes including gas diffusion and heat conduction in fractal porous media [19], fractional-order controller in temperature and motor control applications [20], lateral control of an autonomous guided vehicle [21], and fractional-order HIV-immune system with memory [22]. So, these new types of problems should be well studied and analyzed, and approximate methods for them should be developed effectively [23]. The fractal–fractional optimal control problems (FFOCPs) are a generalization of the FOCPs. Some computational techniques have employed to solve FFOCPs, such as Dehestani and Ordokhani [24] offered a numerical method for resolving FF optimal control and variational problems that is based on the Pell–Lucas polynomials and the pseudo-operational matrix of FF derivative. Heydari et al. [25] used the Legendre polynomials method to numerically solve nonlinear FFOCPs. A numerical method for the FFOCP of a novel malaria mathematical model was proposed by Sweilam et al. [26]. Sabermahani et al. [27] proposed a method based on the generalized Lucas wavelets method for solving nonlinear FFOCPs. Rahimkhani et al. [28] investigated the numerical treatment of 2D FFOCPs by the Müntz–Legendre polynomials method. Liu et al. [29] applied the control parametrization technique for numerically solving FFOCPs involving Caputo-Fabrizio derivatives.

The wavelets have gained popularity in science and engineering as a result of its effective applications in optimal control, signal analysis, numerical analysis, and more. Wavelet techniques offer excellent computational features, including uniform approximation with no accumulative error, handling of singularities, flexibility in managing different boundary conditions of differential equations, and adaptive and iterative techniques for nonlinear systems. The wavelets technique outperforms other methods for solving differential equations numerically. For the benefits of wavelets numerical schemes, see Reference [30]. Many researchers worked on several wavelets for the solutions of FDEs. Some of these wavelets include Haar wavelets [31], Chebyshev wavelets [32], Pell wavelets [33], Bernoulli wavelets [34], Vieta–Fibonacci wavelets [35], Genocchi wavelets [36, 37], and many others.

The Chelyshkov wavelets represent a family of orthonormal wavelet bases derived from the Chelyshkov polynomials. They have demonstrated considerable effectiveness in the numerical resolution of both differential and integral equations. Owing to their inherent orthogonality, structural simplicity, and computational efficiency, the Chelyshkov wavelets are particularly well-suited for a wide range of applications in applied mathematics, scientific computing, and engineering analysis. The Chelyshkov wavelets were previously utilized to solve fractional delay differential equations [38], delay FOCPs [39], distributed-order fractional differential equations [40], and a nonlinear system of ordinary differential equations [41].

In this paper, we incorporate the Chelyshkov wavelets and neural network method for solving the following FFOCPs:

$$\min J = \int_0^T \mathcal{G}(t, \mathcal{X}(t), \mathcal{U}(t))dt, \tag{1}$$

constrained by the nonlinear FF dynamical system

$$D_t^{\gamma,\eta}\mathcal{X}(t) = \mathcal{F}(t, \mathcal{X}(t), \mathcal{U}(t)), \tag{2}$$

and the initial condition

$$\mathcal{X}(0) = \mathcal{X}_0. \tag{3}$$

In this context, $\mathcal{G}$ and $\mathcal{F}$ are given continuous operator, $\mathcal{X}(t)$ and $\mathcal{U}(t)$ are state and control variables, respectively, $T \in \mathbb{R}^+$, $\mathcal{X}_0 \in \mathbb{R}$, and $D^{\gamma,\eta}\mathcal{X}(t)$ represents the Atangana–Riemann–Liouville FF derivative of order (γ, η).

It is worth noting that FOCPs may also involve state and control constraints as well as terminal cost terms. Several well-established approaches have been developed to address such problems, including gradient-based optimization methods and control parameterization techniques (see, for example, [42–44]). In the present work, however, we restrict our attention to unconstrained formulations in order to focus on the numerical treatment of nonlocal memory effects and fractal dynamics.

In fact, in this study, a wavelet-based neural network framework is developed to efficiently solve nonlinear FFOCPs in Equations (1–3). The proposed approach combines the approximation capability of the Chelyshkov wavelets with the flexibility of neural networks to capture the inherent nonlocal memory and fractal characteristics of the underlying dynamical systems. By transforming the original problem into an equivalent variational formulation and employing Gauss–Legendre quadrature, the resulting model is reduced to a system of nonlinear algebraic equations. This system is then solved using Newton's iterative method, providing an accurate and computationally efficient numerical scheme. In general, the advantages of integrating neural networks with the Chelyshkov wavelets are as follows:

- *Efficient representation of complex dynamics*: The Chelyshkov wavelets offer a compact and accurate basis for representing functions, while the neural network learns nonlinear residuals and complex patterns beyond the wavelets approximation, enabling accurate modeling of nonlinear FFOCPs.
- *Separation of global behavior and fine details*: The wavelets basis effectively captures the overall smooth structure of the solution, whereas the neural network adapts to localized variations, discontinuities, and multiscale effects. This separation enhances accuracy without compromising stability.
- *Improved accuracy with moderate computational cost*: Using wavelets alone may require a large number of basis functions to achieve high accuracy. Incorporating the neural network allows further improvement in precision without excessively increasing computational cost.
- *Balance between interpretability and learning capability*: The Chelyshkov wavelets provide a mathematically grounded and interpretable framework, while the neural network contributes the ability to learn complex patterns. Their combination yields a method that is both theoretically analyzable and practically powerful.

To provide an overview of the work, the paper's outline is as follows: some essential definitions, properties, and notations of the FF calculus, the Chelyshkov wavelets and neural network method are presented in Section 2. In Section 3, a novel approach for solving nonlinear FFOCPs has been developed, based on the neural network algorithm and the Chelyshkov wavelets. The convergence of the proposed method is investigated in Section 4. Section 5 provides numerical results that demonstrate the precision and potency of the recently suggested numerical system. Finally, Section 6 consists of a brief summary.

2 | Principles

This section provides essential definitions, properties, and notations of fractal-FC, Chelyshkov wavelets and neural network method that are fundamental to this study.

2.1 | FF Operator

Definition 1 ([18]). Let $\mathcal{X}(t)$ is the continuous and fractal differentiable of order η, the FF derivative in the Atangana–Riemann–Liouville sense of order (γ, η) is defined as follows:

$$D_t^{\gamma,\eta}\mathcal{X}(t) = \frac{B(\gamma)}{1-\gamma}\frac{d}{dt^{\eta}}\int_0^t E_{\gamma}\left(\frac{-\gamma(t-s)^{\gamma}}{1-\gamma}\right)\mathcal{X}(s)ds, \tag{4}$$

where $0 < \gamma, \eta < 1$.

Definition 2 ([18]). Let $\mathcal{X}(t)$ is continuous function, the FF integral in the Atangana–Riemann–Liouville sense of order (γ, η) is defined as follows:

$$I_t^{\gamma,\eta}\mathcal{X}(t) = \frac{\gamma\eta}{B(\gamma)\Gamma(\gamma)}\int_0^t (t-s)^{\gamma-1}s^{\eta-1}\mathcal{X}(s)ds + \frac{\eta(1-\gamma)t^{\eta-1}\mathcal{X}(t)}{B(\gamma)}, \tag{5}$$

where $B(\gamma) = 1-\gamma+\frac{\gamma}{\Gamma(\gamma)}$ and $0 < \gamma, \eta < 1$.

The one-and two-parameter Mittag–Leffler functions are identified respectively as follows [16]

$$E_{\gamma}(t) = \sum_{j=0}^{\infty}\frac{t^j}{\Gamma(j\gamma+1)}, \qquad \gamma \in R^+, t \in R,$$

and

$$E_{\gamma,\nu}(t) = \sum_{j=0}^{\infty}\frac{t^j}{\Gamma(j\gamma+\nu)}, \qquad \gamma, \nu \in R^+, t \in R.$$

Property 1 ([17]). For FF derivative and integral in the Atangana–Riemann–Liouville sense, we have

$$I_t^{\gamma,\eta}D_t^{\gamma,\eta}\mathcal{X}(t) = \mathcal{X}(t) - \mathcal{X}(0).$$

2.2 | Chelyshkov Wavelets

The Chelyshkov wavelets are specified on $L^2[0,1)$ as follows [40]

$$\varphi_{n,m}(t) = \begin{cases} \sqrt{2m+1}2^{\frac{k-1}{2}}\mathcal{P}_{m,\hat{m}}(2^{k-1}t-\hat{n}), & \frac{\hat{n}}{2^{k-1}} \le t < \frac{\hat{n}+1}{2^{k-1}}, \\ 0, & \text{otherwise}, \end{cases} \tag{6}$$

where $m = 0, 1, \dots, \hat{m}$; and $\hat{n} = n-1$; $n = 1, 2, \dots, 2^{k-1}$. Furthermore, the Chelyshkov polynomials, denoted by $\mathcal{P}_{m,\hat{m}}(t)$ are defined as follows over the interval $[0, 1]$ [40]:

$$\mathcal{P}_{m,\hat{m}}(t) = \sum_{r=m}^{\hat{m}}(-1)^{r-m}\binom{\hat{m}-m}{r-m}\binom{\hat{m}+r+1}{\hat{m}-m}t^r, \quad m = 0, 1, \dots, \hat{m}. \tag{7}$$

The following formulation provides the orthogonality criterion for the Chelyshkov polynomials, which are orthogonal over $[0, 1]$ [40]:

$$\int_0^1 \mathcal{P}_{m,\hat{m}}(t)\mathcal{P}_{n,\hat{m}}(t)dt = \frac{\delta_{m,n}}{m+n+1},$$

where $\delta_{m,n}$ is the Kronecker delta.

2.3 | Neural Network Method

In this work, to solve the nonlinear FFOCPs, we present an orthonormal Chelyshkov wavelets neural network (ChWNN). The proposed neural network consists of three layers as follows:

- Input layer: this layer consists of a single input node, denoted as t, which processes $\imath$ input data points given by $\{t_1, t_2, \dots, t_{\imath}\}$.

- Hidden layer: A collection of orthogonal functions is chosen to serve as activation functions in this layer. In particular, we increase the representational capacity of the network by using the orthonormal Chelyshkov wavelets as the activation functions.
- Output layer: The orthonormal Chelyshkov wavelets from the hidden layer are combined linearly to form the input to this layer. This linear combination is subjected to an activation function to produce the final output. Consequently, the ChWNN's output for an input t with parameter set C is written as

$$\mathbb{N}(t,.,C) = ACT(\Phi(t)),$$

where $ACT(.)$ is activation function, and $\Phi(t)$ is given by the following linear combination:

$$\Phi(t) = \sum_{n=1}^{2^{k-1}} \sum_{m=0}^{\hat{m}} c_{n,m}\varphi_{n,m}(t).$$

The vector C is structured as:

$$C = [c_{1,0}, c_{1,1}, \dots, c_{1,\hat{m}}, c_{2,0}, \dots, c_{2,\hat{m}}, \dots, c_{2^{k-1},\hat{m}}]^T.$$

Remark 1. The training data set can be picked using many methodologies, such as equidistant points or the roots of the Legendre polynomial. In this study, the training data set is constructed using the Legendre polynomial's roots.

3 | The Established Strategy

In this part, we create a novel approach to solve the nonlinear FFOCP in Equations (1–3), based on the ChWNN. We apply the operator $I_t^{\gamma,\eta}$ from Definition 2 to both sides of Equation (2) to solve problems (1–3), yielding:

$$\mathcal{X}(t) = \mathcal{X}_0 + I_t^{\gamma,\eta}(\mathcal{F}(t,\mathcal{X}(t),\mathcal{U}(t))). \tag{8}$$

By using the Atangana–Riemann–Liouville FF integral operator formulation, we obtain

$$\begin{aligned}\mathcal{X}(t) = \mathcal{X}_0 &+ \frac{\gamma\eta}{B(\gamma)\Gamma(\gamma)}\int_0^t (t-s)^{\gamma-1}s^{\eta-1}\mathcal{F}(s,\mathcal{X}(s),\mathcal{U}(s))ds \\ &+ \frac{\eta(1-\gamma)t^{\eta-1}}{B(\gamma)}\mathcal{F}(t,\mathcal{X}(t),\mathcal{U}(t)).\end{aligned} \tag{9}$$

Using the Legendre–Gauss quadrature rule [45] for the integral in Equation (9), we derive

$$\begin{aligned}\overline{\mathcal{X}}(t,\mathcal{X}(t)) = \mathcal{X}_0 &+ \frac{t\gamma\eta}{2B(\gamma)\Gamma(\gamma)}\sum_{j=1}^{n^\star}\omega_j\left(t-\left(\frac{t}{2}\tau_j+\frac{t}{2}\right)\right)^{\gamma-1}\left(\frac{t}{2}\tau_j+\frac{t}{2}\right)^{\eta-1} \\ &\times\mathcal{F}\left(\frac{t}{2}\tau_j+\frac{t}{2},\mathcal{X}\left(\frac{t}{2}\tau_j+\frac{t}{2}\right),\mathcal{U}\left(\frac{t}{2}\tau_j+\frac{t}{2}\right)\right) \\ &+ \frac{\eta(1-\gamma)t^{\eta-1}}{B(\gamma)}\mathcal{F}(t,\mathcal{X}(t),\mathcal{U}(t)).\end{aligned} \tag{10}$$

Substituting Equation (10) into Equation (1), yields:

$$\min J = \int_0^T \mathcal{G}(t,\overline{\mathcal{X}}(t,\mathcal{X}(t)),\mathcal{U}(t))dt. \tag{11}$$

Now, we approximate the functions $\overline{\mathcal{X}}(t)$ and $\mathcal{U}(t)$ using the ChWNN as

$$\mathcal{X}(t) \simeq ACT_1\left(\sum_{n=1}^{2^{k-1}}\sum_{m=0}^{\hat{m}} c_{n,m}\varphi_{n,m}(t)\right) = \mathbb{N}_1(t,\mathcal{X},C), \tag{12}$$

and

$$\mathcal{U}(t) \simeq ACT_2\left(\sum_{n'=1}^{2^{k'-1}}\sum_{m'=0}^{\hat{m}'} c'_{n',m'}\varphi_{n',m'}(t)\right) = \mathbb{N}_2(t,\mathcal{U},C'), \tag{13}$$

where $ACT_1(t)$ and $ACT_2(t)$ denote the activation functions in neural network, and $c_{n,m}$ and $c'_{n',m'}$ represent the unknown coefficients. Substituting Equations (12) and (13) in Equation (11), we obtain

$$\min J = \int_0^T \mathcal{G}(t, \overline{\mathcal{X}}(t, \mathbb{N}_1(t,\mathcal{X},C)), \mathbb{N}_2(t,\mathcal{U},C'))dt. \tag{14}$$

We use the Legendre–Gauss quadrature rule [45] as

$$J \simeq \frac{T}{2}\sum_{j=1}^{n^\star}\varpi_j\mathcal{G}\Big(\frac{T}{2}\zeta_j+\frac{T}{2}, \overline{\mathcal{X}}\Big(\frac{T}{2}\zeta_j+\frac{T}{2}, \mathbb{N}_1\Big(\frac{T}{2}\zeta_j+\frac{T}{2},\mathcal{X},C\Big)\Big), \mathbb{N}_2\Big(\frac{T}{2}\zeta_j+\frac{T}{2},\mathcal{U},C'\Big)\Big), \tag{15}$$

where $\{\varpi_j\}_{j=1}^{n^\star}$ and $\{\zeta_j\}_{j=1}^{n^\star}$ are weights and Legendre–Gauss quadrature nodes, respectively.

Lastly, we use the following prerequisites to determine the optimal values of the problem's unknown components:

$$\frac{\partial}{\partial c_{n,m}}J = 0, \quad n = 1,2,\dots,2^{k-1}; m = 0,1,\dots,\hat{m}, \tag{16}$$

and

$$\frac{\partial}{\partial c'_{n',m'}}J = 0, \quad n' = 1,2,\dots,2^{k'-1};'m = 0,1,\dots,\hat{m}'. \tag{17}$$

Finally, we obtain a system of $2^{k-1}\hat{m}+2^{k'-1}\hat{m}'$ algebraic equations with $2^{k-1}\hat{m}+2^{k'-1}\hat{m}'$ unknowns. The above system should be solved to determine $c_{n,m}$ and $c'_{n',m'}$. To this end, Newton's iterative scheme is employed, and the FindRoot package in Mathematica software is utilized for its implementation. Therefore, the approximate solutions for $\mathcal{X}(t)$, $\mathcal{U}(t)$ and J are obtained by determining the unknown coefficients.

4 | Convergence Analysis

The convergence of the suggested method inside the Hilbert space framework is examined in this section. We demonstrate that as the number of the Chelyshkov wavelets basis ($m^\star = 2^{k-1}(\hat{m}+1) = 2^{k'-1}(\hat{m}'+1)$) and number of the Gauss–Legendaire iterations ($n^\star$) increases, the approximate optimal value converges to the exact value. Also, in this work, we consider $\hat{m} = \hat{m}'$, and $k = k'$.

Lemma 1 ([46]). *Assuming that $\mathcal{X}(t), \mathcal{U}(t) \in \mathbb{C}^{\hat{m}+1}[0,1]$ are expanded in terms of the Chelyshkov wavelets, denoted by $\mathcal{X}^\star_{m^\star}(t), \mathcal{U}^\star_{m^\star}(t)$, it follows that*

$$\lim_{m^\star\to\infty}\|\mathcal{X}(.) - \mathcal{X}^\star_{m^\star}(.)\|_2 = 0, \lim_{m^\star\to\infty}\|\mathcal{U}(.) - \mathcal{U}^\star_{m^\star}(.)\|_2 = 0. \tag{18}$$

Lemma 2. *Let $\mathcal{X}^\star_{m^\star}(t)$ is the best approximation to $\mathcal{X}(t)$ in the set spanned by the Chelyshkov wavelets, it follows that*

$$\|I_t^{\gamma,\eta}\mathcal{X}(.) - I_t^{\gamma,\eta}\mathcal{X}^\star_{m^\star}(.)\|_2 \leq \kappa\|\mathcal{X}(.) - \mathcal{X}^\star_{m^\star}(.)\|_2, \tag{19}$$

where $\kappa = \frac{\gamma\eta}{B(\gamma)\Gamma(\gamma)}\sqrt{\frac{\Gamma(2\gamma-1)\Gamma(2\eta-1)}{\Gamma(2\gamma+2\eta-2)(2\gamma+2\eta-2)}} + \frac{(1-\gamma)\eta}{B(\gamma)}$.

Proof. From Equation (2), and the Schwarz's inequality, we acquire

$$\begin{aligned}&|I_t^{\gamma,\eta}(\mathcal{X}(t) - \mathcal{X}^\star_{m^\star}(t))|\\ &\leq \frac{\gamma\eta}{B(\gamma)\Gamma(\gamma)}\int_0^t (t-s)^{\gamma-1}s^{\eta-1}|\mathcal{X}(s) - \mathcal{X}^\star_{m^\star}(s)|ds\end{aligned}$$

$$
\begin{aligned}
&+\frac{(1-\gamma)\eta}{B(\gamma)}t^{\eta-1}|\mathcal{X}(t)-\mathcal{X}^{\star}_{m^{\star}}(t)| \\
&\leq \frac{\gamma\eta}{B(\gamma)\Gamma(\gamma)}\left(\int_0^t (t-s)^{2\gamma-2}s^{2\eta-2}ds\right)^{\frac{1}{2}}\left(\int_0^t (\mathcal{X}(s)-\mathcal{X}^{\star}_{m^{\star}}(s))^2 ds\right)^{\frac{1}{2}} \\
&+\frac{(1-\gamma)\eta}{B(\gamma)}|\mathcal{X}(t)-\mathcal{X}^{\star}_{m^{\star}}(t)| \\
&\leq \frac{\gamma\eta}{B(\gamma)\Gamma(\gamma)}\sqrt{\frac{\Gamma(2\gamma-1)\Gamma(2\eta-1)}{\Gamma(2\gamma+2\beta-2)}}t^{\gamma+\eta-\frac{3}{2}}\|\mathcal{X}(.)-\mathcal{X}^{\star}_{m^{\star}}(.)\|_2 \\
&+\frac{(1-\gamma)\eta}{B(\gamma)}|\mathcal{X}(t)-\mathcal{X}^{\star}_{m^{\star}}(t)|. \qquad (20)
\end{aligned}
$$

Taking L^2-norm on both side of Equation (20), we achieve

$$
\begin{aligned}
&\|I_t^{\gamma,\eta}(\mathcal{X}(.)-\mathcal{X}^{\star}_{m^{\star}}(.))\|_2 \\
&\leq \frac{\gamma\eta}{B(\gamma)\Gamma(\gamma)}\sqrt{\frac{\Gamma(2\gamma-1)\Gamma(2\eta-1)}{\Gamma(2\gamma+2\eta-2)}}\|t^{\gamma+\eta-\frac{3}{2}}\|_2\|\mathcal{X}(.)-\mathcal{X}^{\star}_{m^{\star}}(.)\|_2 \\
&+\frac{(1-\gamma)\eta}{B(\gamma)}\|\mathcal{X}(.)-\mathcal{X}^{\star}_{m^{\star}}(.)\|_2 \\
&\leq \left(\frac{\gamma\eta}{B(\gamma)\Gamma(\gamma)}\sqrt{\frac{\Gamma(2\gamma-1)\Gamma(2\eta-1)}{\Gamma(2\gamma+2\eta-2)(2\gamma+2\eta-2)}}+\frac{(1-\gamma)\eta}{B(\gamma)}\right)\|\mathcal{X}(.)-\mathcal{X}^{\star}_{m^{\star}}(.)\|_2. \qquad (21)
\end{aligned}
$$

□

Theorem 1. *Let $\mathcal{X}^{\star}_{m^{\star}}$ and $\mathcal{U}^{\star}_{m^{\star}}$ be the approximate optimal solutions to $\mathcal{X}(t)$ and $\mathcal{U}(t)$ in the space spanned by the Chelyshkov wavelets. Assume that $\mathcal{F}$ and $\mathcal{G}$ satisfy the Lipschitz condition with constants ℓ_1 and ℓ_2, respectively, then we conclude*

$$
J=\lim_{m^{\star},n^{\star}\to\infty} G_{n^{\star}}(\mathcal{X}^{\star}_{m^{\star}},\mathcal{U}^{\star}_{m^{\star}}), \qquad (22)
$$

where

$$
G_{n^{\star}}(\mathcal{X}^{\star}_{m^{\star}},\mathcal{U}^{\star}_{m^{\star}})=\frac{T}{2}\sum_{j=1}^{n^{\star}}\varpi_j\mathcal{G}(t_j,\mathcal{X}_0+I^{\gamma,\eta}(\mathcal{F}(t_j,\mathcal{X}^{\star}_{m^{\star}}(t_j),\mathcal{U}^{\star}_{m^{\star}}(t_j))),\mathcal{U}^{\star}_{m^{\star}}(t_j)),
$$

and $t_j=\frac{T}{2}\zeta_j+\frac{T}{2}$.

Proof. Since $\mathcal{F}$ and $\mathcal{G}$ satisfy the Lipschitz condition with constants ℓ_1 and ℓ_2, we obtain

$$
\begin{aligned}
&\|\mathcal{G}(.,\mathcal{X}_0+I^{\gamma,\eta}(\mathcal{F}(.,\mathcal{X}(.),\mathcal{U}(.))),\mathcal{U}(.))-\mathcal{G}(.,\mathcal{X}_0+I^{\gamma,\eta}(\mathcal{F}(.,\mathcal{X}^{\star}_{m^{\star}}(.),\mathcal{U}^{\star}_{m^{\star}}(.))),\mathcal{U}^{\star}_{m^{\star}}(.))\|_2 \\
&\leq \ell_1\|I^{\gamma,\eta}\mathcal{F}(.,\mathcal{X}(.),\mathcal{U}(.))-I^{\gamma,\eta}\mathcal{F}(.,\mathcal{X}^{\star}_{m^{\star}}(.),\mathcal{U}^{\star}_{m^{\star}}(.))\|_2+\ell_1\|\mathcal{U}(.)-\mathcal{U}^{\star}_{m^{\star}}(.)\|_2 \\
&\leq \ell_1\kappa\|\mathcal{F}(.,\mathcal{X}(.),\mathcal{U}(.))-\mathcal{F}(.,\mathcal{X}^{\star}_{m^{\star}}(.),\mathcal{U}^{\star}_{m^{\star}}(.))\|_2+\ell_1\|\mathcal{U}(.)-\mathcal{U}^{\star}_{m^{\star}}(.)\|_2 \\
&\leq \ell_1\ell_2\kappa(\|\mathcal{X}(.)-\mathcal{X}^{\star}_{m^{\star}}(.)\|_2+\|\mathcal{U}(.)-\mathcal{U}^{\star}_{m^{\star}}(.)\|_2)+\ell_1\|\mathcal{U}(.)-\mathcal{U}^{\star}_{m^{\star}}(.)\|_2 \\
&\leq \ell_1\ell_2\kappa\|\mathcal{X}(.)-\mathcal{X}^{\star}_{m^{\star}}(.)\|_2+\ell_1(\ell_2\kappa+1)\|\mathcal{U}(.)-\mathcal{U}^{\star}_{m^{\star}}(.)\|_2. \qquad (23)
\end{aligned}
$$

Moreover, since $\mathcal{G}$ is a continuous function, it follows that [47]

$$
\int_0^T \mathcal{G}(t,\mathcal{X}_0+I^{\gamma,\eta}(\mathcal{F}(t,\mathcal{X}(t),\mathcal{U}(t))),\mathcal{U}(t))dt=\lim_{n^{\star}\to\infty}\frac{T}{2}\sum_{j=1}^{n^{\star}}\varpi_j\mathcal{G}(t_j,\mathcal{X}_0+I^{\gamma,\eta}(\mathcal{F}(t_j,\mathcal{X}(t_j),\mathcal{U}(t_j))),\mathcal{U}(t_j)). \qquad (24)
$$

This implies that

$$\begin{aligned}
&\int_0^T \mathcal{G}(t, \mathcal{X}_0 + I^{\gamma,\eta}(\mathcal{F}(t, \mathcal{X}(t), \mathcal{U}(t))), \mathcal{U}(t))dt \\
&= \lim_{m^\star, n^\star \to \infty} \frac{T}{2}\Bigg(\sum_{j=1}^{n^\star} \varpi_j \mathcal{G}(t_j, \mathcal{X}_0 + I^{\gamma,\eta}(\mathcal{F}(t_j, \mathcal{X}^\star_{m^\star}(t_j), \mathcal{U}^\star_{m^\star}(t_j))), \mathcal{U}^\star_{m^\star}(t_j)) \\
&\quad + \sum_{j=1}^{n^\star} \varpi_j \big(\mathcal{G}(t_j, \mathcal{X}_0 + I^{\gamma,\eta}(\mathcal{F}(t_j, \mathcal{X}(t_j), \mathcal{U}(t_j))), \mathcal{U}(t_j)) \\
&\quad - \mathcal{G}(t_j, \mathcal{X}_0 + I^{\gamma,\eta}(\mathcal{F}(t_j, \mathcal{X}^\star_{m^\star}(t_j), \mathcal{U}^\star_{m^\star}(t_j))), \mathcal{U}^\star_{m^\star}(t_j))\big) \Bigg). \qquad (25)
\end{aligned}$$

Based on the uniform convergence of (18) and (19) along with Equation (23), it follows that

$$\begin{aligned}
&\lim_{m^\star, n^\star \to \infty} \Big\| \sum_{j=1}^{n^\star} \varpi_j \big(\mathcal{G}(t_j, \mathcal{X}_0 + I^{\gamma,\eta}(\mathcal{F}(t_j, \mathcal{X}(t_j), \mathcal{U}(t_j))), \mathcal{U}(t_j)) \\
&\quad - \mathcal{G}(t_j, \mathcal{X}_0 + I^{\gamma,\eta}(\mathcal{F}(t_j, \mathcal{X}^\star_{m^\star}(t_j), \mathcal{U}^\star_{m^\star}(t_j))), \mathcal{U}^\star_{m^\star}(t_j))\big) \Big\|_2 \leq 0. \qquad (26)
\end{aligned}$$

Therefore, we conclude

$$\begin{aligned}
&\int_0^T \mathcal{G}(t, \mathcal{X}_0 + I^{\gamma,\eta}(\mathcal{F}(t, \mathcal{X}(t), \mathcal{U}(t))), \mathcal{U}(t))dt \\
&= \lim_{m^\star, n^\star \to \infty} \frac{T}{2} \sum_{j=1}^{n^\star} \varpi_j \mathcal{G}(t_j, \mathcal{X}_0 + I^{\gamma,\eta}(\mathcal{F}(t_j, \mathcal{X}^\star_{m^\star}(t_j), \mathcal{U}^\star_{m^\star}(t_j))), \mathcal{U}^\star_{m^\star}(t_j)). \qquad (27)
\end{aligned}$$

This complete the proof. □

5 | Computational Findings

To assess the accuracy and effectiveness of the developed approach, four test examples are examined. The calculations were created in Mathematica 11 and all required numerical simulations were run on a personal computer. To evaluate the proposed method, absolute error and residual error are used when the exact solution is available and unavailable, respectively. Moreover, stability is examined via small perturbations in the initial conditions, and the value of the cost function is reported as an indicator of solution quality. AE and NR stand for absolute error and numerical results, respectively, in this section.

Example 1. Consider the following nonlinear FFOCP ([24, 25]):

$$\min J = \frac{1}{2}\int_0^1 (\mathcal{X}(t) - \sin(t))^2 + (\mathcal{U}(t) - \tan(t))^2 dt,$$

under the following conditions

$$D^{\gamma,\eta}\mathcal{X}(t) = 3e^{6t}(t^2+2t+9)^2\mathcal{X}(t) + \cos(t)\mathcal{U}^2(t) - 3e^{6t}\sin(t)(t^2+2t+9)^2 - \cos(t)\tan^2(t) + \frac{B(\gamma)t^{2-\eta}}{\eta(1-\gamma)}\sum_{r=0}^{\infty}(-1)^r t^{2r} E_{\gamma,2r+2}\left(\frac{-\gamma t^\gamma}{1-\gamma}\right),$$

and the initial condition

$$\mathcal{X}(0) = 0.$$

The exact solution to the given problem is $(\mathcal{X}(t), \mathcal{U}(t), J) = (\sin(t), \tan(t), 0)$.

TABLE 1 | Comparison of the $AE_{\mathcal{X}}$, $AE_{\mathcal{U}}$ and AE_J for $\gamma = 0.60, \eta = 0.35$ obtained using the adopted strategy with Reference [24] for Example 1.

	Reference [24]		Suggested approach			
	$M = 6$		$k = 2, \hat{m} = 5$		$k = 1, \hat{m} = 10$	
t	$AE_{\mathcal{X}}$	$AE_{\mathcal{U}}$	$AE_{\mathcal{X}}$	$AE_{\mathcal{U}}$	$AE_{\mathcal{X}}$	$AE_{\mathcal{U}}$
0.1	5.12×10^{-5}	3.17×10^{-5}	2.38×10^{-6}	5.21×10^{-7}	1.45×10^{-6}	9.79×10^{-8}
0.2	8.45×10^{-5}	9.10×10^{-5}	1.30×10^{-6}	9.94×10^{-7}	3.00×10^{-6}	8.60×10^{-8}
0.3	8.84×10^{-5}	9.76×10^{-6}	5.17×10^{-6}	1.12×10^{-6}	3.24×10^{-6}	3.76×10^{-8}
0.4	7.34×10^{-5}	8.68×10^{-5}	8.38×10^{-6}	5.73×10^{-6}	2.77×10^{-6}	5.61×10^{-8}
0.5	5.40×10^{-5}	5.97×10^{-6}	4.15×10^{-5}	8.29×10^{-4}	2.12×10^{-6}	1.22×10^{-7}
0.6	3.80×10^{-5}	9.34×10^{-5}	9.25×10^{-6}	7.64×10^{-5}	1.40×10^{-6}	7.44×10^{-8}
0.7	2.53×10^{-5}	1.85×10^{-5}	2.04×10^{-6}	1.92×10^{-5}	9.08×10^{-7}	6.64×10^{-8}
0.8	1.41×10^{-5}	1.17×10^{-4}	2.74×10^{-7}	2.21×10^{-5}	5.94×10^{-7}	2.05×10^{-7}
0.9	1.75×10^{-5}	7.74×10^{-5}	1.04×10^{-6}	1.53×10^{-5}	2.89×10^{-7}	3.20×10^{-7}
AE_J	5.22×10^{-9}		5.60×10^{-25}		4.80×10^{-25}	

TABLE 2 | Comparison of the AE_J obtained using the adopted strategy for $k = 2$ with Reference [25] for Example 1.

	Reference [25]			Suggested approach
t	$n = 4$	$n = 8$	$n = 12$	$\hat{m} = 5$
$\gamma = 0.35, \eta = 0.50$	1.49×10^{-6}	2.12×10^{-11}	1.65×10^{-15}	3.62×10^{-24}
$\gamma = 0.55, \eta = 0.50$	1.49×10^{-6}	2.12×10^{-11}	3.53×10^{-15}	9.61×10^{-25}
$\gamma = 0.75, \eta = 0.50$	1.49×10^{-6}	2.13×10^{-11}	1.47×10^{-14}	4.54×10^{-25}
$\gamma = 0.90, \eta = 0.50$	1.49×10^{-6}	2.40×10^{-11}	7.78×10^{-14}	7.95×10^{-26}
$\gamma = 0.60, \eta = 0.15$	1.49×10^{-6}	2.12×10^{-11}	1.35×10^{-15}	1.12×10^{-25}
$\gamma = 0.60, \eta = 0.35$	1.49×10^{-6}	2.12×10^{-11}	2.73×10^{-15}	5.60×10^{-25}
$\gamma = 0.60, \eta = 0.55$	1.49×10^{-6}	2.12×10^{-11}	5.41×10^{-15}	4.10×10^{-21}
$\gamma = 0.60, \eta = 0.75$	1.49×10^{-6}	2.12×10^{-11}	6.67×10^{-15}	1.03×10^{-24}

The approximate solution of the above problem is expressed as:

$$ACT_1(t) = ACT_2(t) = \sinh(t).$$

In Table 1, we compare the AEs of $\mathcal{X}(t), \mathcal{U}(t), J$ (denoted by $AE_{\mathcal{X}}$, $AE_{\mathcal{U}}$ and AE_J) for $\gamma = 0.60, \eta = 0.35$ obtained using the current approach with those obtained using the Pell–Lucas polynomials method as reported in [24]. Additionally, Table 2 presents a comparison of the AE_J obtained using the proposed method and the Legendre polynomials method [25]. Figure 1 illustrates the AEs and NRs curves for $\mathcal{X}(t)$ and $\mathcal{U}(t)$ for $\gamma = 0.90, \eta = 0.50$ with $k = 1, \hat{m} = 10$. The NRs of $\mathcal{X}(t)$ and $\mathcal{U}(t)$ for $k = 1, \hat{m} = 5$ for different values of γ, η are illustrated in Figure 2.

Example 2. Consider the following nonlinear FFOCP [24]:

$$\min J = \int_0^{\frac{3}{2}} \left(e^{-t} + \sin^2(t)(\mathcal{X}(t) - t^3 - t^5)^2 + e^{-t}(\mathcal{U}(t) - \cos(t))^2\right) dt,$$

under the following conditions

$$D^{\gamma,\eta}\mathcal{X}(t) = -\sin(t)\mathcal{X}(t) + \sin(\mathcal{U}(t)) + (t^3 + t^5)\sin(t) - \sin(\cos(t)) + \frac{B(\gamma)3!t^{4-\eta}}{\eta(1-\gamma)} E_{\gamma,4}\left(\frac{-\gamma t^\gamma}{1-\gamma}\right) + \frac{B(\gamma)5!t^{6-\eta}}{\eta(1-\gamma)} E_{\gamma,6}\left(\frac{-\gamma t^\gamma}{1-\gamma}\right),$$

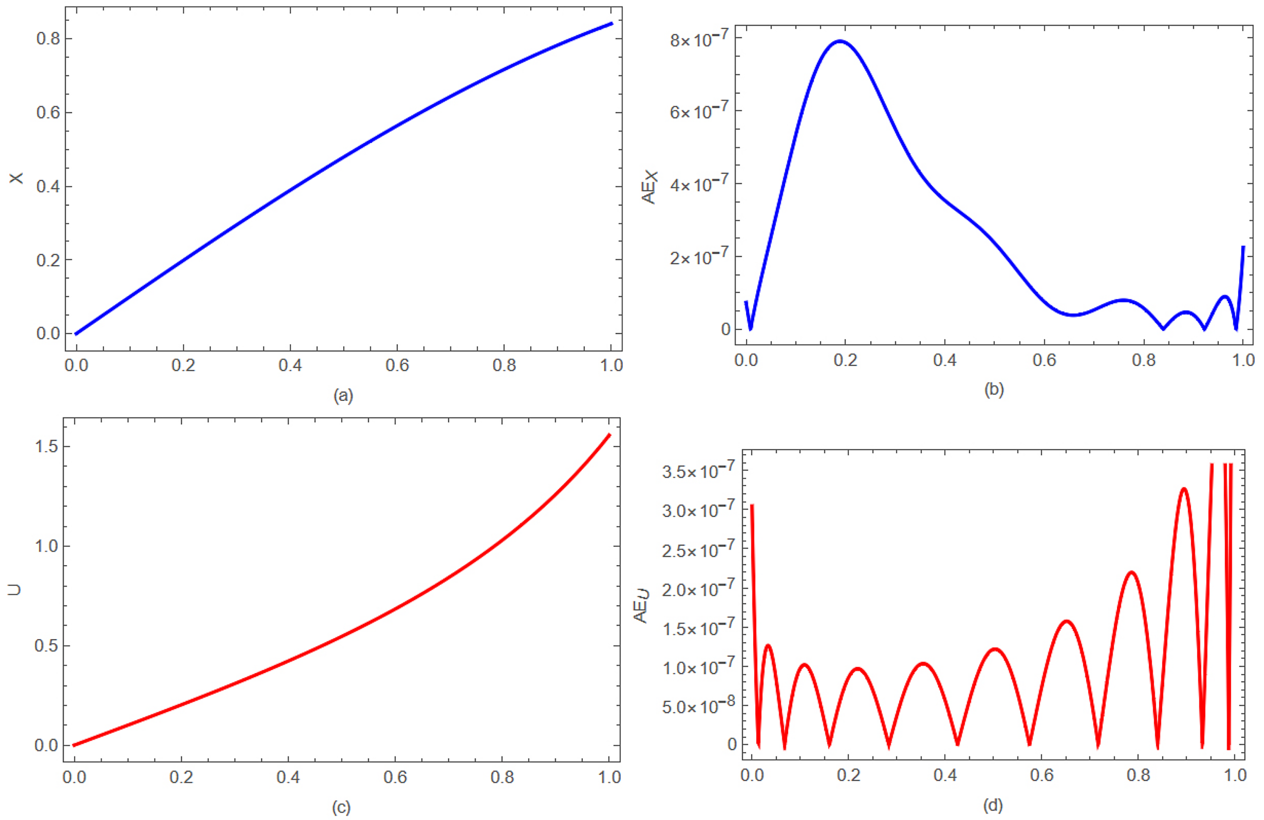

FIGURE 1 | The AEs and NRs of $\mathcal{X}(t)$ and $\mathcal{U}(t)$ for $\gamma = 0.90, \eta = 0.50$ with $k = 1, \hat{m} = 10$ for Ex. 1. [Colour figure can be viewed at wileyonlinelibrary.com]

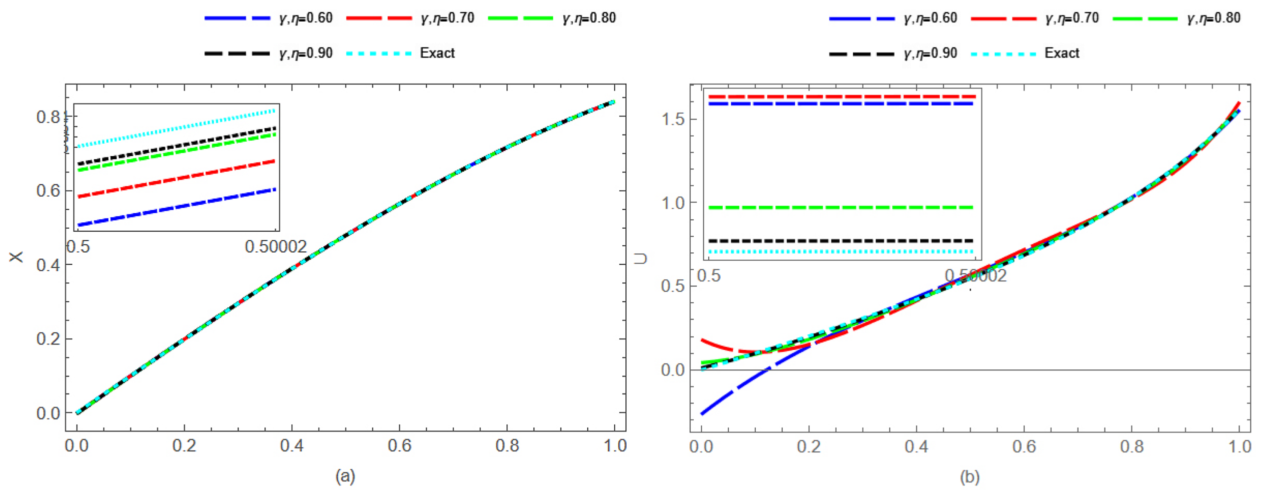

FIGURE 2 | The NRs of $\mathcal{X}(t)$ and $\mathcal{U}(t)$ for $k = 1, \hat{m} = 5$ for Example 1. [Colour figure can be viewed at wileyonlinelibrary.com]

and the initial condition

$$\mathcal{X}(0) = 0.$$

The exact solution to the given problem is $(\mathcal{X}(t), \mathcal{U}(t), J) = (t^3 + t^5, \cos(t), 1 - e^{-\frac{3}{2}})$.

The approximate solution of the above problem is expressed as:

$$ACT_1(t) = t, \quad ACT_2(t) = \sinh(t).$$

TABLE 3 | Comparison of the values and AEs of J obtained using the adopted strategy for $k = 1, \gamma = 0.5$ with Reference [24] for Example 2.

	$\eta = 0.55$		$\eta = 0.15$	
	J	AE_J	J	AE_J
Reference [24]				
$M = 5$	0.7768698401989184	—	0.7768698399230136	—
$M = 8$	0.7768698398515702	—	0.7768698398515702	—
Suggested approach				
$M = 5$	0.7768704862113269	6.46×10^{-7}	0.7768699946009163	1.55×10^{-7}
$M = 8$	0.7768698398693931	1.78×10^{-11}	0.7768698398739181	2.23×10^{-11}
$M = 10$	0.7768698398515467	2.35×10^{-14}	0.7768698398515503	1.98×10^{-14}

TABLE 4 | The AEs of $\mathcal{X}(t)$ and $\mathcal{U}(t)$ obtained using the adopted strategy with $k = 1, \gamma = 0.99$ for Example 2.

	$\eta = 0.25$		$\eta = 0.50$		$\eta = 0.75$	
t	$AE_{\mathcal{X}}$	$AE_{\mathcal{U}}$	$AE_{\mathcal{X}}$	$AE_{\mathcal{U}}$	$AE_{\mathcal{X}}$	$AE_{\mathcal{U}}$
0.1	1.88×10^{-5}	3.88×10^{-8}	1.69×10^{-5}	3.88×10^{-8}	2.03×10^{-5}	3.88×10^{-8}
0.2	8.43×10^{-5}	2.13×10^{-8}	6.29×10^{-5}	2.13×10^{-8}	6.27×10^{-5}	2.13×10^{-8}
0.3	2.05×10^{-4}	9.25×10^{-8}	1.38×10^{-4}	9.25×10^{-8}	1.25×10^{-4}	9.25×10^{-8}
0.4	4.06×10^{-4}	4.31×10^{-8}	2.55×10^{-4}	4.31×10^{-8}	2.14×10^{-4}	4.31×10^{-8}
0.5	7.26×10^{-4}	8.38×10^{-8}	4.32×10^{-4}	8.38×10^{-8}	3.42×10^{-4}	8.38×10^{-8}
0.6	1.22×10^{-3}	5.23×10^{-8}	6.91×10^{-4}	5.23×10^{-8}	5.23×10^{-4}	5.23×10^{-8}
0.7	1.94×10^{-3}	9.22×10^{-8}	1.06×10^{-3}	9.22×10^{-8}	7.73×10^{-4}	9.22×10^{-8}
0.8	2.98×10^{-3}	4.59×10^{-8}	1.58×10^{-3}	4.59×10^{-8}	1.11×10^{-3}	4.59×10^{-8}
0.9	4.44×10^{-3}	1.05×10^{-7}	2.28×10^{-3}	1.05×10^{-7}	1.56×10^{-3}	1.05×10^{-7}
AE_J	2.54×10^{-14}		2.54×10^{-14}		2.54×10^{-14}	

TABLE 5 | Comparison of the AE_J obtained using the adopted strategy for $k = 1$ with Reference [25] for Example 2.

	Reference [25]		Suggested approach		
t	$n = 4$	$n = 8$	$\hat{m} = 5$	$\hat{m} = 7$	$\hat{m} = 10$
$\gamma = 0.25, \eta = 0.55$	8.02×10^{-5}	2.67×10^{-13}	5.04×10^{-7}	3.72×10^{-10}	1.58×10^{-14}
$\gamma = 0.45, \eta = 0.55$	7.56×10^{-5}	3.27×10^{-13}	6.65×10^{-7}	1.11×10^{-10}	2.25×10^{-14}
$\gamma = 0.65, \eta = 0.55$	7.42×10^{-5}	5.40×10^{-13}	4.59×10^{-7}	4.47×10^{-11}	2.48×10^{-14}
$\gamma = 0.85, \eta = 0.55$	1.08×10^{-3}	8.62×10^{-8}	1.98×10^{-7}	4.13×10^{-11}	2.54×10^{-14}
$\gamma = 0.35, \eta = 0.25$	7.57×10^{-5}	2.45×10^{-13}	1.74×10^{-7}	6.27×10^{-10}	1.05×10^{-14}
$\gamma = 0.35, \eta = 0.45$	7.70×10^{-5}	3.19×10^{-13}	3.24×10^{-7}	3.14×10^{-10}	1.70×10^{-14}
$\gamma = 0.35, \eta = 0.65$	7.91×10^{-5}	2.10×10^{-13}	9.76×10^{-7}	1.57×10^{-10}	2.12×10^{-14}
$\gamma = 0.35, \eta = 0.85$	8.17×10^{-5}	3.26×10^{-14}	1.78×10^{-6}	8.24×10^{-11}	2.32×10^{-14}

In Table 3, the estimated values and AEs of J obtained using the adopted strategy for $k = 1, \gamma = 0.5$ are compared with the Pell–Lucas polynomials method [24]. The AEs of $\mathcal{X}(t)$, $\mathcal{U}(t)$ and J obtained using the formulated technique with $k = 1, \gamma = 0.99$ and $\eta = 0.25, 0.50, 0.75$ are reported in Table 4. Moreover, Table 5 compares the values of AE_J obtained using the proposed method with those obtained using the Legendre polynomials method [25]. Figure 3 presents the AEs and NRs curves for $\mathcal{X}(t)$ and $\mathcal{U}(t)$ with $k = 1, \hat{m} = 10, \gamma = 0.95, \eta = 0.85$. Figure 4 illustrates the NRs of $\mathcal{X}(t)$ and $\mathcal{U}(t)$ for $k = 1, \hat{m} = 6$, evaluated at different values of γ and η.

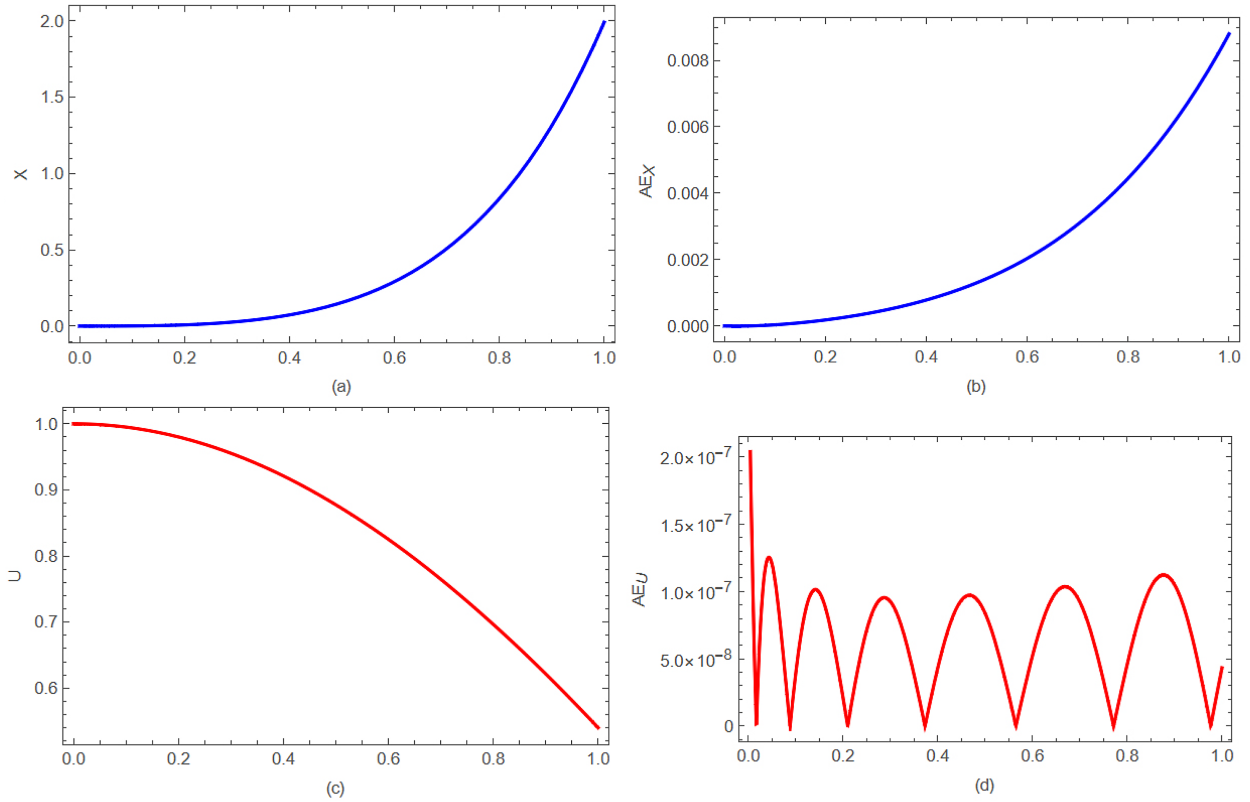

FIGURE 3 | The AEs and NRs of $\mathcal{X}(t)$ and $\mathcal{U}(t)$ with $k = 1, \hat{m} = 10, \gamma = 0.95, \eta = 0.85$ for Example 2. [Colour figure can be viewed at wileyonlinelibrary.com]

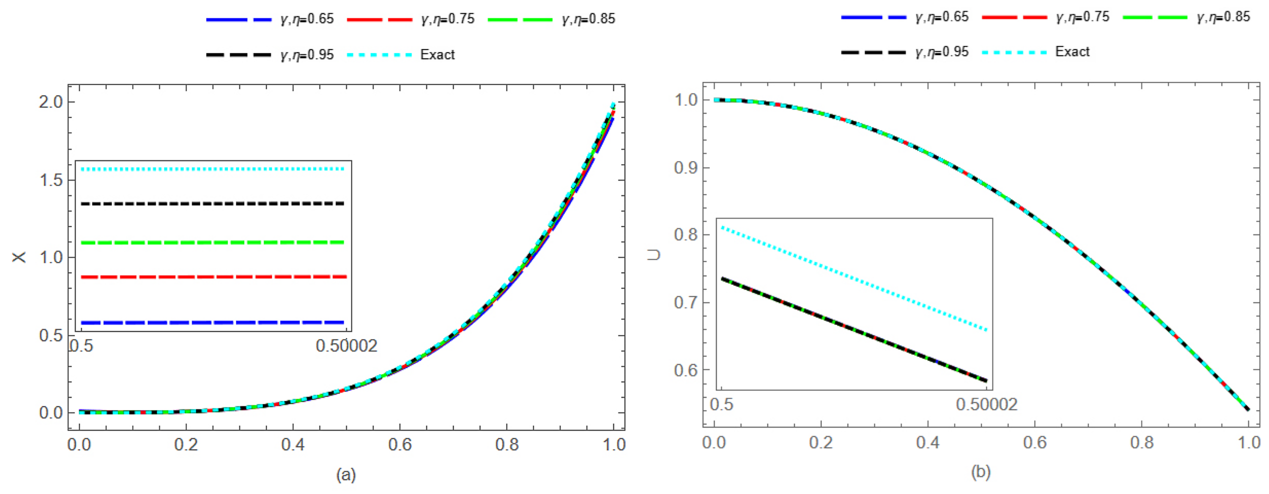

FIGURE 4 | The NRs of $\mathcal{X}(t)$ and $\mathcal{U}(t)$ for $k = 1, \hat{m} = 6$ for Example 2. [Colour figure can be viewed at wileyonlinelibrary.com]

Example 3. Consider the following nonlinear FFOCP:

$$\min J = \int_0^1 (\mathcal{X}(t) - e^{-t})^2 + (\mathcal{U}(t) - te^{-t} + \frac{1}{2}e^{t^2-t})^2 dt,$$

under the following conditions

$$D^{\gamma,\eta}\mathcal{X}(t) = \mathcal{X}^2(t) + 2e^t\mathcal{U}(t) + \frac{B(\gamma)t^{1-\eta}}{\eta(1-\gamma)}\sum_{r=0}^{\infty}(-1)^r E_{\gamma,r+1}\left(\frac{-\gamma t^\gamma}{1-\gamma}\right)$$
$$- e^{-2t} - 2e^t\left(te^{-t} - \frac{1}{2}e^{t^2-t}\right),$$

TABLE 6 | The AEs of J obtained using the adopted strategy for $k = 2$ and different values of γ, η for Example 3.

γ, η	$\hat{m} = 10$	$\hat{m} = 11$
$\gamma = \eta = 0.1$	8.16×10^{-26}	1.89×10^{-27}
$\gamma = \eta = 0.3$	4.93×10^{-27}	3.22×10^{-30}
$\gamma = \eta = 0.5$	1.44×10^{-25}	5.90×10^{-30}
$\gamma = \eta = 0.7$	1.66×10^{-18}	4.97×10^{-30}
$\gamma = \eta = 0.9$	1.54×10^{-26}	1.87×10^{-32}

TABLE 7 | The AEs of J obtained using the adopted strategy for $k = 1$ and different values of γ, η for Example 4.

γ, η	$\hat{m}_1 = \hat{m}_2 = 1$	$\hat{m}_1 = \hat{m}_2 = 2$	$\hat{m}_1 = \hat{m}_2 = 3$
$\gamma = \eta = 0.25$	3.08×10^{-33}	3.97×10^{-31}	4.85×10^{-31}
$\gamma = \eta = 0.35$	0	4.83×10^{-31}	8.74×10^{-32}
$\gamma = \eta = 0.45$	0	4.95×10^{-31}	1.19×10^{-30}
$\gamma = \eta = 0.55$	0	8.98×10^{-32}	9.06×10^{-32}
$\gamma = \eta = 0.65$	0	4.84×10^{-31}	6.68×10^{-32}
$\gamma = \eta = 0.75$	3.08×10^{-33}	4.33×10^{-31}	2.73×10^{-31}
$\gamma = \eta = 0.85$	3.08×10^{-33}	4.70×10^{-32}	3.82×10^{-33}
$\gamma = \eta = 0.95$	1.79×10^{-30}	9.68×10^{-32}	2.92×10^{-31}

and the initial condition

$$\mathcal{X}(0) = 1.$$

The exact solution to the given problem is $(\mathcal{X}(t), \mathcal{U}(t), J) = \left(e^{-t}, te^{-t} - \frac{1}{2}e^{t^2-t}, 0\right)$.

The approximate solution of the above problem is expressed as:

$$ACT_1(t) = ACT_2(t) = t.$$

Table 6 displays the AEs of J resulting from the developed approach for $k = 2$ and different values of γ, η.

Example 4. Consider the following nonlinear 2D-FFOCP:

$$\min J = \int_0^1 \int_0^1 (\mathcal{X}(x,t) - e^{-t}\sin(x))^2 + (\mathcal{U}(x,t) - (t^2+t)x^2)^2 dx dt,$$

under the following conditions

$$\begin{aligned} D_t^{\gamma,\eta}\mathcal{X}(x,t) = {} & 2\mathcal{X}(x,t) + \sin(t)\mathcal{U}(x,t) + \frac{B(\gamma)t^{1-\eta}}{\eta(1-\gamma)}\sum_{r=0}^{\infty}(-1)^r E_{\gamma,r+1}\left(\frac{-\gamma t^{\gamma}}{1-\gamma}\right)\sin(x) \\ & - 2e^{-t}\sin(x) - (t^2+t)x^2, \end{aligned}$$

and the initial condition

$$\mathcal{X}(x,0) = \sin(x).$$

The exact solution to the given problem is $(\mathcal{X}(x,t), \mathcal{U}(x,t), J) = (e^{-t}\sin(x), (t^2+t)x^2, 0)$.

The approximate solution of the above problem is expressed as:

$$ACT_1(t) = ACT_2(t) = \sinh(t).$$

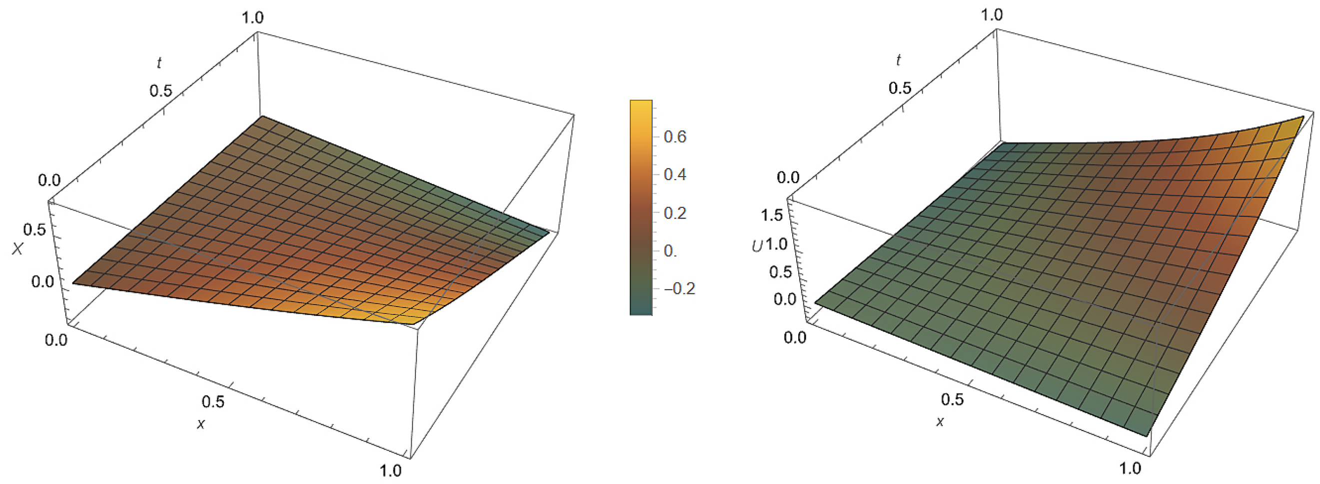

FIGURE 5 | The NRs of $\mathcal{X}(x,t)$ and $\mathcal{U}(x,t)$ with $k=1, \hat{m}_1=\hat{m}_2=2, \gamma=\eta=0.55$ for Example 4. [Colour figure can be viewed at wileyonlinelibrary.com]

Table 7 shows the AEs of J resulting from the developed approach for $k=1$ and different values of γ, η. Figure 5 illustrates the NRs of $\mathcal{X}(x,t)$ and $\mathcal{U}(x,t)$ with $k=1, \hat{m}_1=\hat{m}_2=2, \gamma=\eta=0.55$.

6 | Concluding Remarks

In this work, we introduced a novel model for FFOCPs that uses the Atangana–Riemann–Liouville framework. To tackle such issues numerically, the ChWNN method was utilized. First, the topic under consideration was converted into an equivalent variational problem using the definition of the FF integral. The problem was then transformed into an algebraic equation system using the Chelyshkov wavelets, the neural network approach, and Gauss–Legendre integration. Finally, the system was solved using Newton's iterative approach. Furthermore, a convergence analysis of the proposed approach was performed. The experimental results from the test instances demonstrated that the proposed numerical methods were accurate, had high precision, and required minimal processing. We compared our approximations to the exact results and those obtained from other methods. The method presented in this research proved to be accurate and effective, and it could be applied to locate and investigate numerical solutions for a wide range of real-world models. We plan to do the following works in the future:

- Developing adaptive and optimized neural network architectures to enhance computational efficiency, especially for large-scale problems.
- Exploring hybrid approaches by combining the proposed method with other numerical or machine learning techniques, such as physics-informed neural networks or genetic algorithms, to further enhance accuracy and efficiency.
- Applying the methodology to practical problems in engineering, physics, biology, or finance where nonlocal and memory-dependent behaviors are significant.
- Stability analysis of the suggested scheme for the numerical approximation of the problem under study is another interesting problem for future research.

Author Contributions

Parisa Rahimkhani: conceptualization, data curation, investigation, software, writing – original draft. **Seydi Battal Gazi Karakoc:** conceptualization, data curation, investigation, software, writing – original draft. **Thabet Abdeljawad:** conceptualization, investigation, writing – original draft.

Acknowledgments

We express our sincere thanks to the anonymous referees for valuable suggestions that improved the paper.

Funding

The authors have nothing to report.

Conflicts of Interest

The authors declare no conflicts of interest.

Data Availability Statement

Data will be made available on reasonable request.

References

1. R. L. Bagley and P. J. Torvik, "A Theoretical Basis for the Application of Fractional Calculus to Viscoelasticity," *Journal of Rheology* 27, no. 3 (1983): 201–210.

2. R. L. Magin, "Fractional Calculus in Bioengineering," *Critical Reviews in Biomedical Engineering* 32, no. 1 (2004): 1–104.

3. R. T. Baillie, "Long Memory Processes and Fractional Integration in Econometrics," *Journal of Econometrics* 73, no. 1 (1996): 5–9.

4. F. Mainardi, "Fractional Calculus: Some Basic Problems in Continuum and Statistical Mechanics," in *Fractals and Fractional Calculus in Continuum Mechanics* (Springer Vienna, 1997), 291–348.

5. Y. A. Rossikhin and M. V. Shitikova, "Applications of Fractional Calculus to Dynamic Problems of Linear and Nonlinear Hereditary Mechanics of Solids".

6. S. G. Samko, A. A. Kilbas, and O. I. Marichev, *Fractional Integrals and Derivatives: Theory and Applications* (Gordon and Breach, 1993).

7. V. Kiryakova, *Generalized Fractional Calculus and Applications* (Longman, Harlow and Wiley, 1994).

8. A. Atangana, "Fractal–Fractional Differentiation and Integration: Connecting Fractal Calculus and Fractional Calculus to Predict Complex System," *Chaos, Solitons & Fractals* 102 (2017): 396–406.

9. Z. Li, Z. Liu, and M. A. Khan, "Fractional Investigation of Bank Data With Fractal–Fractional Caputo Derivative," *Chaos, Solitons & Fractals* 131 (2020): 109528.

10. A. Atangana and S. Jain, "Models of Fluid Flowing in Non-Conventional Media: New Numerical Analysis," *Discrete and Continuous Dynamical Systems - Series S* 13, no. 3 (2020): 467–484.

11. W. Wang and M. A. Khan, "Analysis and Numerical Simulation of Fractional Model of Bank Data With Fractal-Fractional Atangana–Baleanu Derivative," *Journal of Computational and Applied Mathematics* 369 (2020): 112646.

12. A. Atangana and S. Qureshi, "Modeling Attractors of Chaotic Dynamical Systems With Fractal–Fractional Operators," *Chaos, Solitons & Fractals* 123 (2019): 320–337.

13. H. M. Srivastava and K. M. Saad, "Numerical Simulation of the Fractal–Fractional Ebola Virus," *Fractal and Fractional* 4, no. 4 (2020): 49.

14. M. Hosseininia, M. H. Heydari, and Z. Avazzadeh, "The Numerical Treatment of Nonlinear Fractal–Fractional 2d Emden–Fowler Equation Utilizing 2d Chelyshkov Polynomials," *Fractals* 28, no. 8 (2020): 2040042.

15. S. İ. Araz, "Numerical Analysis of a New Volterra Integro-Differential Equation Involving Fractal–Fractional Operators," *Chaos, Solitons & Fractals* 130 (2020): 109396.

16. P. Rahimkhani, S. Sedaghat, and Y. Ordokhani, "An Effective Computational Solver for Fractal–Fractional 2D Integro-Differential Equations," *Journal of Applied Mathematics and Computing* 70, no. 4 (2024): 3411–3440.

17. A. Rayal and S. R. Verma, "Numerical Analysis of Pantograph Differential Equation of the Stretched Type Associated With Fractal-Fractional Derivatives via Fractional Order Legendre Wavelets," *Chaos, Solitons & Fractals* 139 (2020): 110076.

18. P. Rahimkhani, Y. Ordokhani, and S. Sabermahani, "Numerical Solution of Fractal–Fractional Differential Equations System via Vieta–Fibonacci Polynomials Fractal–Fractional Integral Operators," *International Journal of Numerical Modelling: Electronic Networks, Devices and Fields* 37, no. 5 (2024): e3283.

19. M. Zamani, M. Karimi-Ghartemani, and N. Sadati, "FOPID Controller Design for Robust Performance Using Particle Swarm Optimization," *Fractional Calculus and Applied Analysis* 10, no. 2 (2007): 169–187.

20. G. W. Bohannan, "Analog Fractional Order Controller in Temperature and Motor Control Applications," *Journal of Vibration and Control* 14, no. 9–10 (2008): 1487–1498.

21. J. I. Suarez, B. M. Vinagre, and Y. Chen, "A Fractional Adaptation Scheme for Lateral Control of an AGV," *Journal of Vibration and Control* 14, no. 9–10 (2008): 1499–1511.

22. Y. Ding, Z. Wang, and H. Ye, "Optimal Control of a Fractional-Order HIV-Immune System With Memory," *IEEE Transactions on Control Systems Technology* 20, no. 3 (2011): 763–769.

23. Z. Gong, C. Liu, K. L. Teo, S. Wang, and Y. Wu, "Numerical Solution of Free Final Time Fractional Optimal Control Problems," *Applied Mathematics and Computation* 405 (2021): 126270.

24. H. Dehestani and Y. Ordokhani, "An Optimum Method for Fractal–Fractional Optimal Control and Variational Problems," *International Journal of Dynamics and Control* 11, no. 1 (2023): 229–241.

25. M. H. Heydari, A. Atangana, and Z. Avazzadeh, "Numerical Solution of Nonlinear Fractal–Fractional Optimal Control Problems by Legendre Polynomials," *Mathematical Methods in the Applied Sciences* 44, no. 4 (2021): 2952–2963.

26. N. H. Sweilam, S. M. Al-Mekhlafi, and A. Almutairi, "Fractal Fractional Optimal Control for a Novel Malaria Mathematical Model; A Numerical Approach," *Results in Physics* 19 (2020): 103446.

27. S. Sabermahani, Y. Ordokhani, and P. Rahimkhani, "Application of Generalized Lucas Wavelet Method for Solving Nonlinear Fractal-Fractional Optimal Control Problems," *Chaos, Solitons & Fractals* 170 (2023): 113348.

28. P. Rahimkhani, Y. Ordokhani, and S. Sedaghat, "The Numerical Treatment of Fractal-Fractional 2D Optimal Control Problems by Müntz–Legendre Polynomials," *Optimal Control Applications and Methods* 44, no. 6 (2023): 3033–3051.

29. C. Liu, X. Yi, Z. Gong, and M. Han, "The Control Parametrization Technique for Numerically Solving Fractal–Fractional Optimal Control Problems Involving Caputo–Fabrizio Derivatives," *Journal of Computational and Applied Mathematics* 472 (2026): 116814.

30. P. Rahimkhani and Y. Ordokhani, "Numerical Investigation of Distributed-Order Fractional Optimal Control Problems via Bernstein Wavelets," *Optimal Control Applications and Methods* 42, no. 1 (2021): 355–373.

31. A. Ali, T. Minamoto, R. Shah, and K. Nonlaopon, "A Novel Numerical Method for Solution of Fractional Partial Differential Equations Involving the Ψ-Caputo Fractional Derivative," *AIMS Mathematics* 8, no. 1 (2023): 2137–2153.

32. D. Zhou, A. Babaei, S. Banihashemi, H. Jafari, J. Alzabut, and S. P. Moshokoa, "A Chebyshev Collocation Approach to Solve Fractional Fisher-Kolmogorov-Petrovskii–Piskunov Equation With Nonlocal Condition," *Fractal and Fractional* 6, no. 3 (2022): 160.

33. S. Sabermahani, P. Rahimkhani, and Y. Ordokhani, "Pell Wavelet-Optimization Procedure for Two Classes of Fractional Partial Differential Equations With Nonlocal Boundary Conditions," *Journal of Computational Science* 90 (2025): 102655.

34. P. Rahimkhani and Y. Ordokhani, "A Numerical Scheme Based on Bernoulli Wavelets and Collocation Method for Solving Fractional Partial Differential Equations With Dirichlet Boundary Conditions," *Numerical Methods for Partial Differential Equations* 35, no. 1 (2019): 34–59.

35. T. Hoseini, Y. Ordokhani, and P. Rahimkhani, "Numerical Solution of Two-Dimensional Fractional Optimal Control Problems Using Fractional Vieta–Fibonacci Wavelets," *International Journal of Systems Science* 57, no. 1 (2026): 259–283.

36. H. Dehestani, Y. Ordokhani, and M. Razzaghi, "On the Applicability of Genocchi Wavelet Method for Different Kinds of Fractional-Order Differential Equations With Delay," *Numerical Linear Algebra with Applications* 26, no. 5 (2019): e2259.

37. P. Rahimkhani and T. Abdeljawad, "Application of χ-Fractional Genocchi Wavelets for Solving χ-Fractional Differential Equations," *Mathematics and Computers in Simulation* 239 (2026): 790–804.

38. F. Mohammadi, "Numerical Solution of Systems of Fractional Delay Differential Equations Using a New Kind of Wavelet Basis," *Computational and Applied Mathematics* 37, no. 4 (2018): 4122–4144.

39. L. Moradi, F. Mohammadi, and D. Baleanu, "A Direct Numerical Solution of Time-Delay Fractional Optimal Control Problems by Using Chelyshkov Wavelets," *Journal of Vibration and Control* 25, no. 2 (2019): 310–324.

40. P. Rahimkhani, Y. Ordokhani, and P. M. Lima, "An Improved Composite Collocation Method for Distributed-Order Fractional Differential Equations Based on Fractional Chelyshkov Wavelets," *Applied Numerical Mathematics* 145 (2019): 1–27.

41. S. C. Shiralashetti, P. I. Kulkarni, and S. I. Hanaji, "Chelyshkov Wavelet-Based Numerical Technique for the Solution of Darcy-Forchheimer Flow of Erying-Powell Radiated Dusty Fluid Over a Stretching Sheet With Cattaneo-Christov Heat Flux," *Numerical Heat Transfer, Part B: Fundamentals* 86, no. 8 (2025): 2691–2720.

42. C. Liu, R. Loxton, K. L. Teo, and S. Wang, "Optimal State-Delay Control in Nonlinear Dynamic Systems," *Automatica* 135 (2022): 109981.

43. Z. Gong, C. Liu, K. L. Teo, and Y. Wu, "A Gradient-Based Optimization Algorithm to Solve Optimal Control Problems With Conformable Fractional-Order Derivatives," *Journal of Computational and Applied Mathematics* 454 (2025): 116169.

44. X. Yi, Z. Gong, C. Liu, H. T. Cheong, K. L. Teo, and S. Wang, "A Control Parameterization Method for Solving Combined Fractional Optimal Parameter Selection and Optimal Control Problems," *Communications in Nonlinear Science and Numerical Simulation* 141 (2025): 108462.

45. Y. Kumar, S. Singh, N. Srivastava, A. Singh, and V. K. Singh, "Wavelet Approximation Scheme for Distributed Order Fractional Differential Equations," *Computers & Mathematics with Applications* 80, no. 8 (2020): 1985–2017.

46. Y. Ordokhani, S. Sabermahani, and P. Rahimkhani, "Application of Chelyshkov Wavelets and Least Squares Support Vector Regression to Solve Fractional Differential Equations Arising in Optics and Engineering," *Mathematical Methods in the Applied Sciences* 48, no. 2 (2025): 1996–2010.

47. M. Y. Hussaini and T. A. Zang, *Spectral Methods in Fluid Dynamics* (Nasa Langley Research Center, 1986).